Translational Oncology 64 (2026) 102659

Contents lists available at ScienceDirect

Translational Oncology

journal homepage: www.elsevier.com/locate/tranon

Original Research

A serum-derived 3D tumor model platform for personalized prediction and monitoring of chemotherapeutic response in pancreatic ductal adenocarcinoma

Sara Cherradi [a,1], Salomé Roux [a,1], Marie Dupuy [b], Eric Assenat [b], Hong Tuan Duong [a,*]

[a] PredictCan Biotechnologies, Biopôle Euromédecine, Grabels, France
[b] Service d'Oncologie Médicale, Hôpital Saint Eloi, Centre Hospitalier Universitaire de Montpellier, Montpellier, France

ARTICLE INFO

Keywords:
Chemotherapy
Clinical response prediction
Personalized care
Patient-derived model

ABSTRACT

Pancreatic ductal adenocarcinoma (PDAC) remains a highly lethal cancer, largely due to late diagnosis, tumor heterogeneity, and a dense, immunosuppressive stroma that limits therapeutic efficacy. While regimens like FOLFIRINOX and gemcitabine-based therapies offer some benefit, treatment selection remains empirical, with no reliable predictive models to guide personalized decisions. We adapted our previously validated serum-derived educated spheroid technology creating 3D spheroids using PDAC patient serum. These spheroids maintained structural integrity, viability, and consistent size over eight days, avoiding overgrowth. They also exhibited extracellular matrix deposition such as type I collagen, and expressed key genes involved in drug resistance and tumor progression including *COL1A1, FN1, MMP2, CXCL1*, and *CXCL2*. Using the Target-Independent Cell Killing (TICK) strategy, we established individualized chemograms to assess true therapeutic response helping clinicians in refining the optimal treatment protocol. In a 16-case study, our model achieved high concordance with clinical responses across gemcitabine, Gem-Pac, and FOLFIRINOX treatments supporting its utility in personalized care. Finally, we demonstrated that predictive accuracy was highest when patient serum was collected within a short window prior to treatment initiation. These findings support PDAC patient serum-educated spheroids as a rapid, non-invasive, and physiologically relevant tool for guiding personalized chemotherapy and monitoring treatment response in real time.

Introduction

Pancreatic ductal adenocarcinoma (PDAC) is the 12th most common cancer and the 7th leading cause of cancer death worldwide [1]. Risk factors for PDAC included genetics such as BRCA1/2, PALB2, or CDKN2A, lifestyle such as smoking, obesity, diabetes, and heavy alcohol use, and chronic pancreatitis [1–3]. For clinical decision-making, PDAC is generally categorized into resectability-based stages including resectable, locally advanced, and metastatic [4]. Delayed diagnosis and early systemic dissemination are key contributors to the poor prognosis of PDAC [5,6]. Furthermore, the tumor's highly desmoplastic and immunosuppressive microenvironment poses significant barriers to effective therapeutic intervention [7]. Neoadjuvant chemotherapy for PDAC used in borderline resectable or locally advanced are FOLFIRINOX, a combination of 5-FU, leucovorin, irinotecan, and oxaliplatin, or gemcitabine + nab-paclitaxel (Gem-Pac)[8]. For metastatic patients, first line chemotherapy is FOLFIRINOX, or Gem-Pac, for those who do not tolerate FOLFIRINOX regimen, or gemcitabine alone for physically weak and elderly ones. Despite advances in chemotherapy regimens, there remains no universally accepted consensus on the optimal treatment strategy for PDAC, particularly in the neoadjuvant and metastatic settings. Indeed, while regimens such as FOLFIRINOX and gemcitabine-based treatments have demonstrated some limited efficacy, the choice of therapy often varies depending on patient condition, molecular profile, and local practice patterns. Thus, in the absence of clear predictive biomarkers, treatment remains largely empirical [8–10].

Abbreviations: PDAC, pancreatic ductal adenocarcinoma; HSC, hepatic stellate cells; PSC, pancreatic stellate cells; Gem-Pac, gemcitabine-paclitaxel; PDO, patient-derived organoid; TICK, target-independent cell killing; CAF, cancer-associated fibroblast; ECM, extracellular matrix.

* Corresponding author.
E-mail address: ht.duong@predictcan.com (H.T. Duong).

[1] These authors contributed equally.

https://doi.org/10.1016/j.tranon.2025.102659
Received 1 October 2025; Received in revised form 15 November 2025; Accepted 18 December 2025
Available online 6 January 2026

Therefore, to improve outcomes in PDAC, it is imperative to develop predictive platforms such as patient-derived *in vitro* models, that can mirror clinical responses. Such tools will help clinicians to tailor treatment strategies prior to therapy initiation and will also assist pharmaceutical developers in identifying and optimizing more effective chemotherapeutic candidates.

Given the aggressive and treatment-resistant nature of PDAC, there is a critical need for robust *in vitro* models to support drug development and clinical decision-making [11]. Presently, existing models often fail to mirror clinical outcomes with high fidelity, primarily due to their inability to capture the desmoplastic stroma, tumor heterogeneity, and adaptive resistance mechanisms observed in patients [11–15]. *In vitro* models commonly used in the PDAC setting include traditional 2D cell lines such as Panc-1, MIA PaCa-2, or BxPC-3, cell line-based spheroids as mono or co-cultures, and patient-derived organoids (PDOs) generated from patient's primary cells [15,16]. Each model offers distinct advantages and limitations in modeling tumor behavior and therapeutic response [17]. To date, PDOs are the most promising system as they retain patient-specific genetics and phenotypes and thus could potentially reproduce individual patient response to chemotherapy [15,16]. However, the implementation of PDOs in real-time clinical decision-making remains constrained by the need for extended culture periods of several weeks, inconsistent establishment rates of 60 to 80 %, and the requirement for specialized resources and expertise that limit their feasibility for routine use in personalized medicine [18,19]. Furthermore, culturing primary tumor cells outside their native environment often leads to changes in their behavior and drug responsiveness. For instance, Hachey and colleagues have reported that tissue-derived primary colorectal cancer cells were sensitive to chemotherapy although clinically the patient was not responding to the treatment emphasizing that drug responses observed *in vitro* may not always align with clinical outcomes [20].

We have recently developed and reported a patient serum-derived educated spheroid technology. We applied this technology in the hepatocellular carcinoma setting, where it demonstrated high accuracy in predicting treatment outcomes, as evidenced by multiple case reports [21]. Building on the inherent flexibility and translational potential of this technology, we adapted it for use in PDAC by establishing a PDAC patient serum-derived educated spheroid model. We exploited the previously validated target-independent cell killing (TICK) exclusion strategy to determine true therapeutic response to chemotherapy. This system enables the investigation of personalized chemotherapy responses, offering an emerging and promising tool for functional precision oncology in PDAC.

Materials and methods

Biological samples, cell lines, and reagents

Patient's blood was collected and processed according to the protocol described elsewhere [22]. Blood samples from healthy donors were obtained from the Etablissement Français du Sang (EFS) Hauts de France-Normandie. The research protocol was conducted under French legal guidelines and fulfilled the requirements of the local institutional ethics committee. Blood samples from PDAC patients were obtained from the CHU of Toulouse, and of Montpellier, FRANCE. For the CHU of Montpellier, samples were provided by the Biological Resource Center of Montpellier University Hospital (BB-0033–00,031 Montpellier). Informed consent was obtained from all subjects and/or their legal guardian(s).

For the CHU of Toulouse, patients' samples were obtained after informed consent in accordance with the Declaration of Helsinki and stored at the « CRB Cancer des Hôpitaux de Toulouse (BB-0033–00,014) » collection. According to the French law, CRB Cancer collection has been declared to the Ministry of Higher Education and Research (DC-2020–4074) and obtained a transfer agreement (AC-2020–4031) after approbation by ethical committees. Clinical and biological annotations of the samples have been declared to the CNIL (Comité National Informatique et Libertés)".

Irinotecan, fluorouracil, oxaliplatin, leucovorin, gemcitabine and paclitaxel were purchased from TargetMol (Linz, Austria).

Pancreatic cells (PANC-1) and monocyte (THP-1) lines were from ATCC (Molsheim, France). Hepatic stellate cell line (TWNT-1) was from Glow Biologics (Tarrytown, NY, USA). Cell culture reagents were provided by StemCell (Saint Égrève, France). Pancreatic cells, monocytes, and hepatic stellate cells were conditioned for a minimum of 2 weeks in MammoCult® basal medium (StemCell) before use to sensitize them to cell educating technology. PDAC and healthy serum-derived educated spheroids were generated and cultured in hSELS medium (PredictCan Biotechnologies, Grabels, France) supplemented with depleted human serum prepared accordingly to our proprietary in-house protocol.

PDAC patient serum-derived spheroids generation and treatments

Educated spheroids were generated from a co-culture of PANC-1 and TWNT-1 in ultra-low attachment plates, using blood sera from healthy donors or from PDAC patients. The system is supplemented with educated monocyte-derived macrophages and dendritic cells and then cultured for 3 days before being treated for 3 days with different concentrations of FOLFIRINOX, gemcitabine, or gemcitabine plus paclitaxel (Gem-Pac). Drugs constituting FOLFIRINOX and Gem-Pac were combined in the following molar ratios: FOLFIRINOX:1.00 irinotecan, 80.95 fluorouracil, 0.80 oxaliplatin, 1.07 leucovorin; Gem-Pac: 1.00 gemcitabine, 0.04 paclitaxel. Importantly, educated spheroids, educated macrophages, and educated dendritic cells were prepared from the same donor/patient, and co-cultured together. Cell viability was then measured at 3 days post-treatment.

ATP quantification and cell viability

ATP quantification/cell viability was measured using CellTiterGlo (Promega, Charbonnières-les-Bains, France) according to the manufacturer's instructions. Briefly, cell viability was evaluated using the CellTiterGlo Luminescent Cell Viability Assay, which quantifies intracellular ATP levels as an indicator of metabolically active cells. After the designated treatment period, the assay reagent was added directly to the cell culture wells to induce lysis and generate a stable luminescent signal proportional to ATP content. Luminescence was recorded using a microplate luminometer (Berthold Tristar 3, Berthold Technologies GmbH & Co, Bad Wildbad, Germany) according to the manufacturer's recommendations.

Background-subtracted luminescent values were used as a surrogate for viable cell number, and viability for each condition was calculated by normalizing the luminescence of treated wells to the corresponding control.

Determination of the target-independent cell killing (TICK) and therapeutic efficacy

For TICK calculation, educated healthy spheroids were treated with gemcitabine, Gem-Pac, or FOLFIRINOX with concentrations up to 1 mM, 2 mM, and 20 μM, respectively. The cell viability was then measured after 3 days of treatment. For each drug, we generated an inhibitory dose-response curve fit with constraints and calculated the $LogIC_{50}$ and HillSlope values. The TICK was calculated using the formula:

$$TICK = 10 \wedge (- ((\mathrm{Log}((100/99) - 1)/\mathrm{HillSlope}) - \mathrm{LogIC}_{50}))$$

For therapeutic efficacy, PDAC patient serum-derived educated spheroids were prepared and then treated with gemcitabine, Gem-Pac, or FOLFIRINOX for 3 days. Inhibitory dose-response curve fits were generated as above. The therapeutic efficacy for each drug and each HCC patient was determined based on the TICK value of the

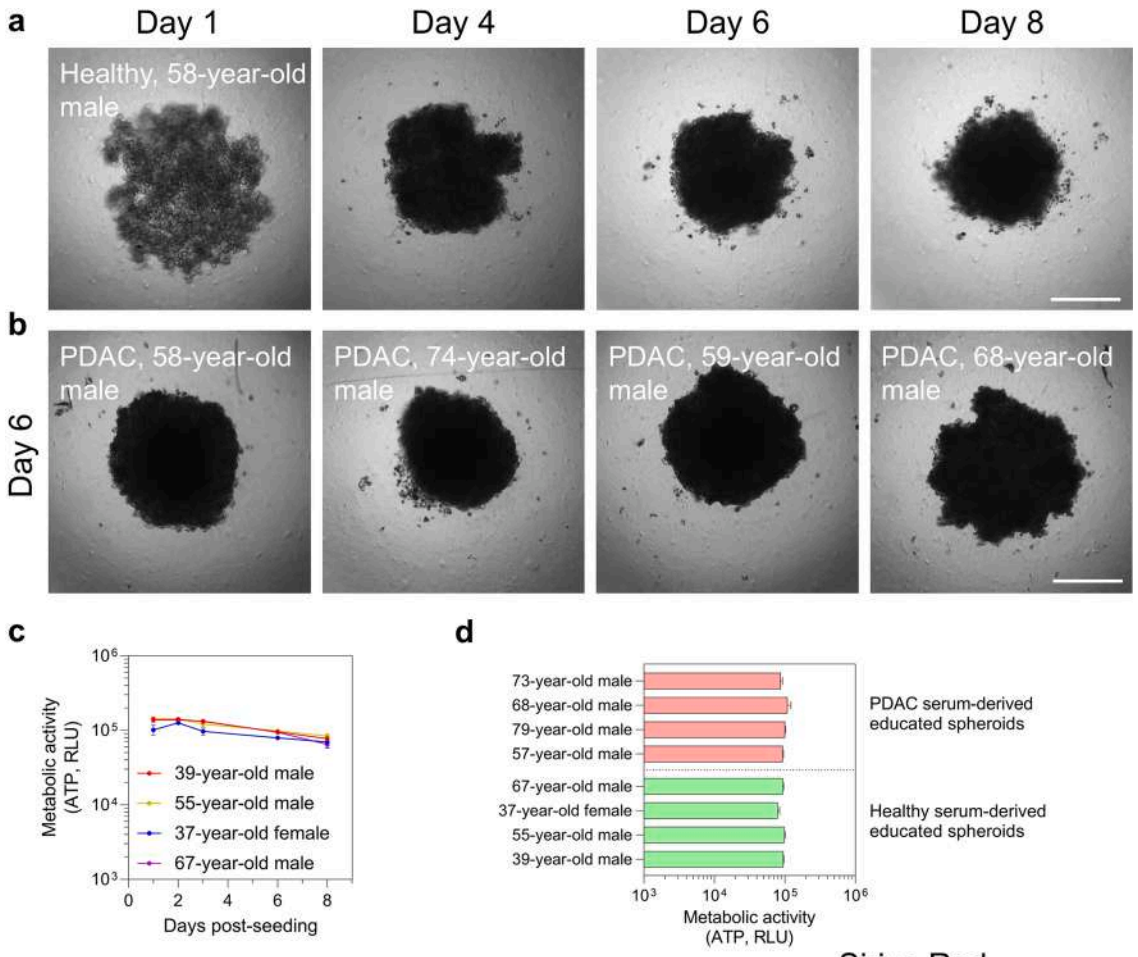

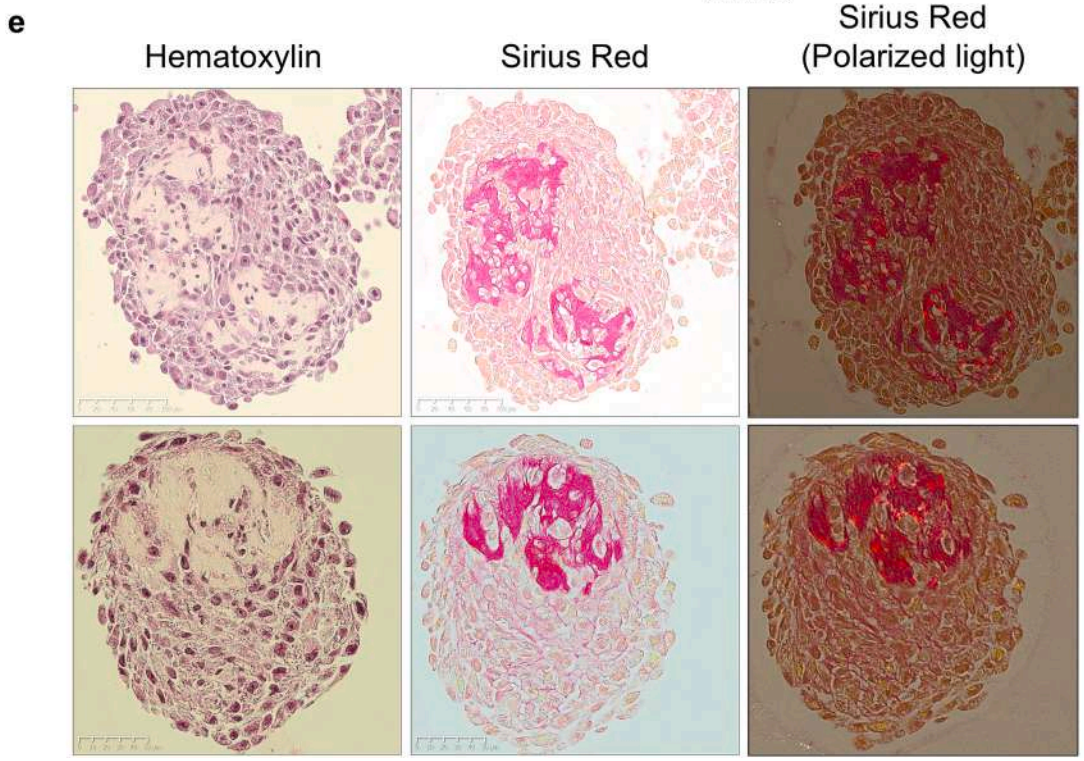

(caption on next page)

Fig. 1. PDAC patient serum-derived educated spheroids show structural integrity without overgrowth, and exhibit ECM deposition. (a) Control of absence of cell overgrowth in cell line-based spheroids cultured with human sera. Light microscopy showing multicellular spheroid formation and growth up to 8 days. Scale bar represents 200 μm. Healthy serum-derived educated spheroids generated from serum of a 58-year-old male donor. Spheroid morphology was monitored for 8 days. Full compaction was reached by day 4 and maintained through day 8. (b) PDAC serum-derived educated spheroids were generated using blood serum from four PDAC patients (a 58-year-old male, a 74-year-old male, a 59-year-old male, and a 68-year-old male). Light microscopy shows that spheroid size at day 6 was comparable to that of healthy serum-derived educated spheroids, indicating an absence of cellular overgrowth. Scale bar represents 200 μm. (c) Stable metabolic activity visualized by ATP quantification in spheroids cultured in blood sera from 4 healthy subjects. The metabolic activity of healthy serum-derived educated spheroids was assessed on days 1, 2, 3, 6, and 8 by quantifying ATP levels using the CellTiterGlo assay. Relative luminescence units (RLU) are shown, reflecting ATP content and thus cellular metabolic activity. Each time point was done in triplicate, and data are shown as mean ± *s*.d. (d) Comparison of ATP levels in healthy spheroids and PDAC spheroids at day 6. The metabolic activity of PDAC serum-derived educated spheroids was assessed on day 6 by quantifying ATP levels using the CellTiterGlo assay. Relative luminescence units (RLU) are shown, reflecting ATP content and thus cellular metabolic activity. Each condition was done in triplicate. Results are expressed as mean ± *s*.d. Bar plots depict ATP levels measured at day 6 in four healthy serum-derived educated spheroids and four PDAC serum-derived educated spheroids, demonstrating comparable metabolic activity in both conditions. (e) Structural integrity and ECM deposition in PDAC patient serum-derived educated spheroids. Representative image of PDAC serum-derived educated spheroids generated from a 71-year-old female metastatic patient, cultured for 6 days, and stained with Hematoxylin and Sirius Red. Observations were made under light microscopy and polarized light.

corresponding drug. A decrease of cell viability before the TICK value means that the drug is efficient on this patient, and a drop of the cell viability above the TICK value means that the drug is inefficient on this patient.

Quantitative PCR

RNA extraction was performed using RNeasy Mini Kit (QIAGEN) according to manufacturer's instructions. Reverse transcription was performed using OneScript® RT Mix for qPCR w/gDNAOut (Ozyme) followed by an amplification with ONEGreen® FAST qPCR Premix (Ozyme) according to manufacturer's instructions. Primers (COL1A1, COL3A1, FN, ACTA2, MMP2, MMP9, IL6, CXCL1, CXCL2 and RRP36) were purchased from BIORAD. Quantitative PCR was performed on an IVDR-compliant thermal cycler (Thermo Fisher Scientific, QuantStudio 5 Dx Real-Time PCR System). All CTs were collected and the ΔCTs were calculated by subtracting to RRP36 (housekeeping gene) CT. Relative expression to RRP36 for each gene was calculated by using the formula $RE = 2^{-\Delta CT}$.

Immunohistochemistry

Paraffin inclusion, sectioning, and staining (Hematoxylin and Sirius Red) of PDAC patient serum-derived educated spheroids were performed by the "Réseau d'Histologie Expérimentale de Montpellier" - RHEM facility in Montpellier, France. Briefly, spheroids were fixed in 4 % formaldehyde and embedded in paraffin prior to sectioning. Serial sections of 4–5 μm thickness were prepared. For morphological assessment, sections were deparaffinized, rehydrated, and stained with Hematoxylin to visualize general tissue architecture, cell morphology, and spheroid organization. To assess collagen deposition, sections were stained with Sirius Red, which specifically binds to fibrillar collagen, allowing qualitative and quantitative evaluation of extracellular matrix content.

After staining, sections were dehydrated, cleared, and mounted with a permanent mounting medium (Permount, Fisher Scientific, France). Stained sections were imaged using a light microscope, and images were captured for subsequent analysis. Histological features, including spheroid structure, cellular density, and collagen distribution, were evaluated to characterize tissue organization and extracellular matrix composition within the spheroids.

Data visualization and analysis

Data visualization was performed using GraphPad Prism v9 (Dotmatics, San Diego, *CA*). Violin plots were used to represent the distribution and density of individual data points, highlighting variability within groups. Nonlinear curve fitting was applied to model relationships between variables and to assess trends over a continuous range. Box plots were used to summarize the median, interquartile range, and overall spread of the data. Bar graphs were used to display group means or percentages for comparison between conditions. These graphical approaches allowed clear representation of both distributional and summary characteristics of the data.

Results

PDAC patient serum-derived educated spheroids maintain structural integrity, exhibit ECM deposition, and express key genes involved in chemotherapy response

In spheroid models, monitoring the absence of overgrowth is essential to preserve the physiological 3D architecture and maintain consistent gradients of nutrients, oxygen, and drug penetration. Indeed, excessive growth can lead to uncontrolled size and necrotic core formation, which can confound the interpretation of chemotherapy response [23,24]. Thus, ensuring stable spheroid dimensions is needed for reproducible and biologically relevant assessment of treatment effects. We generated spheroids supplemented with sera from 4 healthy donors (female, 37-year-old; female, 56-year-old; male, 39-year-old; male, 55-year-old) and monitored their morphology and metabolic activity over an 8-day culture period. We observed that spheroids were already formed and compacted by day 4 (Fig. 1a) and they maintained a stable size without evidence of overgrowth up to day 8. Consistently, ATP quantification revealed stable levels suggesting preserved viability and functionality throughout the observation period (Fig. 1c). We have also generated spheroids supplemented with sera from 4 PDAC patients and assessed their morphology at day 6. As expected, these spheroids did not exhibit cell overproliferation during the study time and displayed a similar diameter to that of spheroids supplemented with healthy serum (Fig. 1b). ATP quantification revealed stable levels in PDAC spheroids, comparable to those in healthy spheroids, confirming their viability and functionality (Fig. 1d).

Next, we assessed the influence of cancer-associated fibroblasts

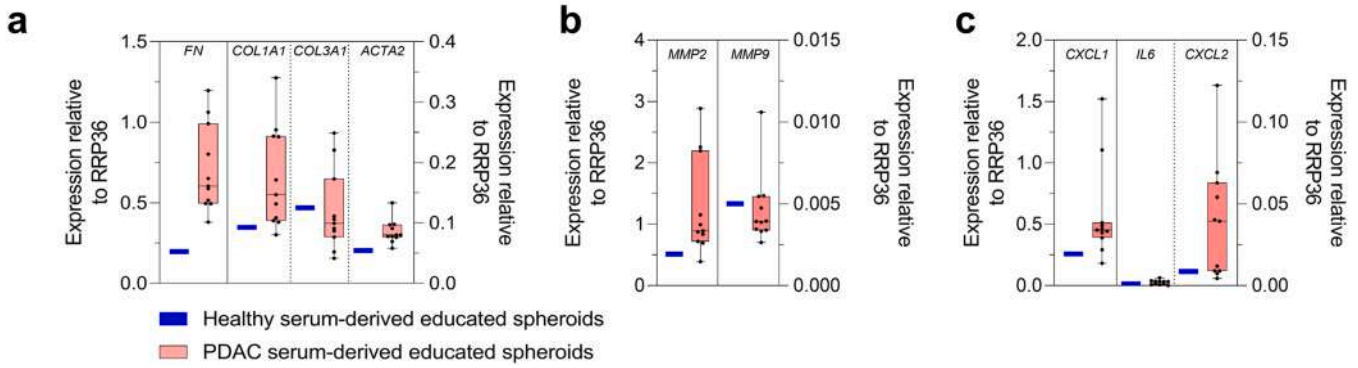

Fig. 2. PDAC patient serum-derived educated spheroids express highly key genes that are involved in the regulation of chemotherapy response as compared to healthy serum-derived educated spheroids. PDAC patient serum-derived educated spheroids were generated using blood serum from 11 PDAC patients or from a healthy blood serum for healthy serum-derived educated spheroids. The expression of key genes involved in the regulation of chemotherapy response including *FN, COL1A1, COL3A1, ACTA2, MMP2, MMP9, CXCL1, IL6*, and *CXCL2*, was quantified by qPCR in PDAC spheroids and in healthy serum-derived educated spheroids, and the resulting expression levels were compared to those of healthy serum-derived educated spheroids. Results are expressed as relative expression to the housekeeping gene RRP36 and compared to a healthy serum-derived educated spheroid condition. (a) Box plots show that *FN, COL1A1*, and *ACTA2* are expressed at higher levels in PDAC serum-derived educated spheroids compared with healthy serum-derived educated spheroids, whereas *COL3A1* expression remains unchanged. (b) Box plots showing increased *MMP2* expression in PDAC serum-derived educated spheroids compared with healthy serum-derived educated spheroids, while *MMP9* expression remains unchanged. Elevated *MMP2* is notable in PDAC due to its role in extracellular matrix degradation, invasion, and tumor aggressiveness. (c) Box plots showing increased *CXCL1* and *CXCL2* expression in PDAC serum-derived educated spheroids compared with the healthy serum-derived condition, while IL6 expression remains unchanged. These data provide insight into how the serum-derived environment modulates inflammatory signaling within spheroids.

(CAFs) on chemotherapy response by measuring extracellular matrix (ECM) deposition within PDAC tumors. PDAC patient serum-derived educated spheroids were generated with blood sera from PDAC patients, stained for hematoxylin to visualize overall cell and tissue architecture (Fig. 1e, left panel) and Sirius Red to monitor collagen deposition as a marker of ECM accumulation (Fig. 1e, middle panel). We observed a well-preserved cellular organization highlighted by hematoxylin staining. Moreover, Sirius Red staining demonstrated collagen deposition, confirming ECM accumulation within the PDAC patient serum-derived educated spheroids. Observation under polarized light further revealed that the deposited matrix was predominantly composed of type I collagen, consistent with the desmoplastic stroma typically found in PDAC (Fig. 1e, right panel). We then analyzed the expression of ECM proteins like fibronectin, type 1 and 3 collagen, matrix metalloproteinases, and chemokines in 11 PDAC patient serum-derived educated spheroids by qPCR as these molecules contribute significantly to the tumor's ability to invade surrounding tissues, to evade immune surveillance, and to resist therapies. As expected, we found a heterogeneous expression of fibronectin (FN), collagen type I (COL1A1), matrix metalloproteinase 2 (MMP2), and the chemokines CXCL1 and CXCL2 across the PDAC patient cohort. Notably, the expression levels of these genes were found to be higher in PDAC patient serum-derived educated spheroids compared to healthy donor serum-derived educated spheroid condition, suggesting that tumor-derived factors in the patient serum may contribute to the expression of these key genes, potentially influencing the response to chemotherapies (Fig. 2).

TICK exclusion-based chemogram generation for personalized drug response profiling in PDAC

It is well known that distinguishing off-target effects on normal cells from on-target effects on cancer cells is crucial to accurately assess a drug's true therapeutic efficacy [25,26]. Indeed, off-target toxicity may cause harm on non-cancerous cells without truly contributing to cancer cell killing leading to misleading results. We previously demonstrated in the context of hepatocellular carcinoma that applying the TICK exclusion strategy enables accurate monitoring of true therapeutic efficacy. Here, we extend this approach to pancreatic ductal adenocarcinoma. TICK values for each treatment regimen such as gemcitabine, Gem-Pac, and FOLFIRINOX, were determined for their off-target effects using a cohort of 24 healthy individuals with ages ranging from 18 to 68 years-old (Fig. 3a). For each individual, a dose-response curve was generated, and TICK value was calculated. We found a wide dispersion of the TICK value within cohorts treated with gemcitabine, Gem-Pac, and FOLFIRINOX, reflecting substantial biological heterogeneity (Fig. 3b). This variation may reduce the reliability of a fixed threshold for stratifying responders and non-responders, potentially leading to misclassification and an increased incidence of false positive or false negative predictions. To reduce misclassification associated with the use of an imprecise TICK cut-off, we implemented a refinement strategy by restricting the analysis to individuals older than 50 years. This selection is justified by the epidemiology of PDAC, which primarily affects older adults [27]. We found that TICK values for gemcitabine, Gem-Pac, and FOLFIRINOX were 143.61 μM, 55.50 μM, and 39.53 nM, respectively (Fig. 3c).

The efficiency of PDAC treatment guidelines, particularly regarding choosing between FOLFIRINOX, Gem-Pac, or gemcitabine alone, is backed by solid clinical trial data. However, in real world practice outcomes may be less favorable than in clinical trials, primarily due to patient heterogeneity such as advanced age, comorbidities, and poor performance status, that affects both treatment tolerance and response. Thus, the implementation of a personalized chemogram in conjunction with existing treatment guidelines may enhance clinical decision-making by enabling more precise regimen selection, ultimately improving therapeutic outcomes and reducing avoidable adverse effects. Applying our TICK exclusion strategy, we generated chemogram for 4 patients with metastatic PDAC, assessing their treatment responses to gemcitabine, Gem-Pac, and FOLFIRINOX in order to evaluate individualized drug sensitivity (Fig. 3d). Among the four metastatic PDAC patients tested, one patient (71-year-old female) showed no response to

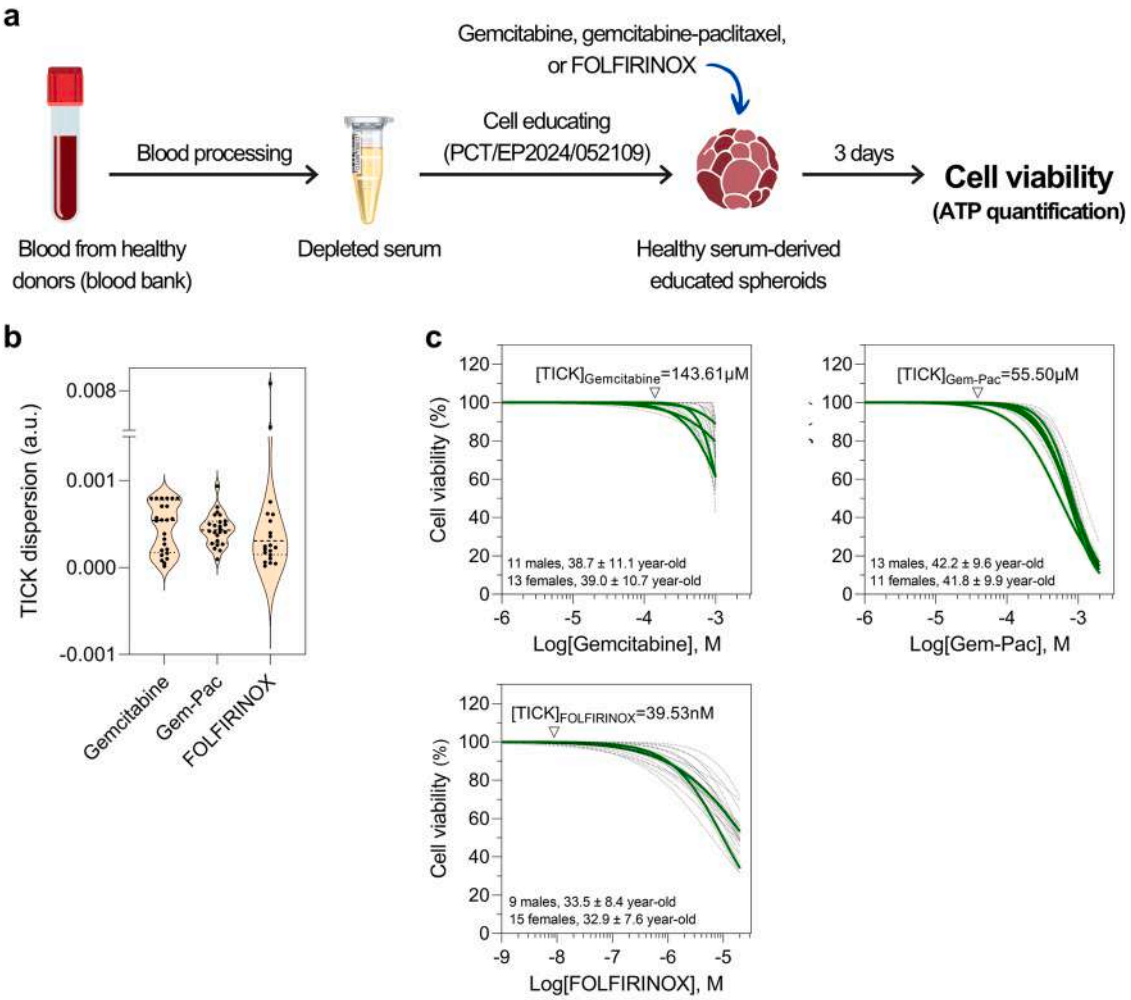

(caption on next page)

Fig. 3. Assessment of the target-independent cell killing (TICK) for each chemotherapeutic agent and illustration of chemogram establishment in four PDAC patients. (a) Schematic workflow showing the key steps prior to obtaining healthy serum-derived educated spheroids, the treatment period, and the endpoint measurement of cell viability. (b) Spheroids were generated using depleted blood sera from 24 healthy individuals. Spheroids were then treated with gemcitabine, Gem-Pac, or FOLFIRINOX. Cell viability was measured at day 3 post-treatment. For each chemotherapy, an inhibitory dose-response curve fit was drawn. Each condition was performed in triplicate for each individual. TICK value was calculated for each individual as the first percentage of cell death. Violin plots show TICK values dispersion within each cohort of individuals treated with gemcitabine alone, Gem-Pac, or FOLFIRINOX. (c) Refinement of TICK determination by restricting the analysis to individuals older than 50 years. Nonlinear curve fitting performed on 24 healthy serum-derived educated spheroids to determine target-independent cell killing (TICK) values for each chemotherapy. Curves corresponding to donors older than 50 years, which were used for TICK calculation, are highlighted in green. Nine drug doses and a control condition were included in this analysis, and all conditions were assayed in technical triplicate. (d) Chemograms of 4 PDAC patients evaluating the response to gemcitabine, Gem-Pac, and FOLFIRINOX. PDAC serum-derived educated spheroids were generated using blood serum from four metastatic PDAC patients and treated for 3 days with different chemotherapies. Cell viability was measured to evaluate the effect of each treatment. A decrease in cell viability at or below the TICK value for each chemotherapy is considered an on-target effect, thereby confirming the true therapeutic efficacy of the drug. Results are expressed as mean % of cell viability ± *s*.e.m. Each condition was performed in technical triplicate.

gemcitabine, Gem-Pac, or FOLFIRINOX. Two patients (69-year-old female and 66-year-old male) were sensitive to both gemcitabine monotherapy and the Gem-Pac combination, with no apparent advantage observed from the addition of paclitaxel. The 69-year-old female patient with metastatic PDAC also exhibited a slight sensitivity to FOLFIRINOX treatment. One PDAC patient (82-year-old female) responded to gemcitabine monotherapy but not to the Gem-Pac combination. This observation may reflect differences in tumor cell treatment tolerance at the cellular level. Indeed, tumor cells can exhibit resistance mechanisms such as drug efflux, enhanced DNA repair, or survival pathway activation, that reduce the effectiveness of combination therapies. Notably, increased tumor cell treatment tolerance is often observed in elderly patients, driven by both cellular and systemic factors associated with aging [28–30], that potentially contribute to poorer responses with more aggressive regimens. Taking together, we demonstrated that using a TICK exclusion strategy on PDAC patient serum-derived educated spheroids, one could establish a personalized chemogram for each patient helping in refining the optimal treatment protocol.

Assessing the performance of patient serum-derived educated spheroids in recapitulating clinical responses to chemotherapy

Although patient-derived primary tumor cell models have been extensively developed and have demonstrated robustness in elucidating tumor biology, evidence supporting a concordance between their predicted therapeutic responses and actual clinical outcomes remains limited, thereby constraining their utility in personalized medicine. We challenged our PDAC patient serum-derived educated spheroids in 16 case studies. In these studies, we aimed to evaluate the performance of our patient serum-derived educated spheroid system and to investigate the impact of blood sampling timing on the system's ability to accurately recapitulate clinical outcomes. To this end, blood samples were collected at different times: more than one month before, more than one week before, or within one week prior to the initiation of the clinical treatment protocol. Blood sera were then prepared and used to generate patient serum-derived educated spheroids. These spheroids were subsequently treated with either gemcitabine alone, Gem-Pac, or FOLFIRINOX, in accordance with the clinical regimen the patient was scheduled to receive or had already received (Fig. 4a). Among the 7 PDAC patients who received gemcitabine monotherapy, our *in vitro* system identified 6 as non-responders, consistent with their clinical outcomes. One patient, a 72-year-old male, showed a slight response to gemcitabine *in vitro*, but this response was not reflected in the clinical setting (Fig. 4b). Additionally, three patients received Gem-Pac treatment. Interestingly, two of them were identified as non-responders both *in vitro* and clinically, while one patient, a 72-year-old female, demonstrated sensitivity to Gem-Pac *in vitro* matching her clinical response (Fig. 5a). Finally, the remaining 6 PDAC patients received FOLFIRINOX. All six were identified as non-responders *in vitro* correlating with their lack of clinical response (Fig. 5b). Taken together, among the 16 PDAC patients analyzed, we observed a single mismatch between the *in vitro* results and clinical outcomes, representing one false positive.

Interestingly, when we analyzed the results based on the timing of blood sampling, we found that the blood sample from the 72-year-old male who received gemcitabine monotherapy, whose *in vitro* response did not match the clinical outcome, had been collected more than one month prior to treatment initiation. In contrast, data derived from blood samples collected less than one month before or after treatment initiation showed full concordance between *in vitro* responses and clinical outcomes (Fig. 6). These findings underscore the importance of collecting blood samples shortly before the start of therapy to maximize the predictive accuracy of the *in vitro* system. Moreover, the observation that post-treatment serum samples also yielded results consistent with clinical responses suggests that the patient serum-derived educated spheroid system may have potential, as a minimally invasive tool, for monitoring drug response or the development of drug resistance during treatment.

Discussion

In this study, we established a simple and non-invasive method to generate personalized PDAC patient serum-educated spheroids. This model provides a physiologically relevant platform to assess actual therapeutic responses thanks to our TICK exclusion strategy and to construct individualized chemogram, potentially guiding treatment decisions in a clinically meaningful way. To the best of our knowledge, this is the first *in vitro* study to demonstrate case-level concordance between spheroid-based drug response profiles and observed clinical outcomes in PDAC patients. These findings highlight the translational potential of our approach in supporting personalized oncology and improving therapeutic decision-making for this aggressive cancer type.

This method was originally developed to assess drug-induced liver injury [22,31,32], but its flexibility has allowed application to hepatocellular carcinoma, where case studies showed its potential to support clinical decision-making [21]. Building on this experience, we explored whether the approach could be adapted for PDAC, presenting an initial, exploratory evaluation in this new context. Although these early findings are encouraging, not all predictive tests ultimately achieve clinical utility, and a gap often exists between research and routine patient care. This underscores the need for additional data and highlights the importance of an exploratory study, which enables assessment of feasibility, establishment of biological and clinical plausibility, detection of early predictive signals, and refinement of methodological parameters. Taking this stepwise approach reduces the risk of launching a large, costly prospective trial without sufficient justification, while

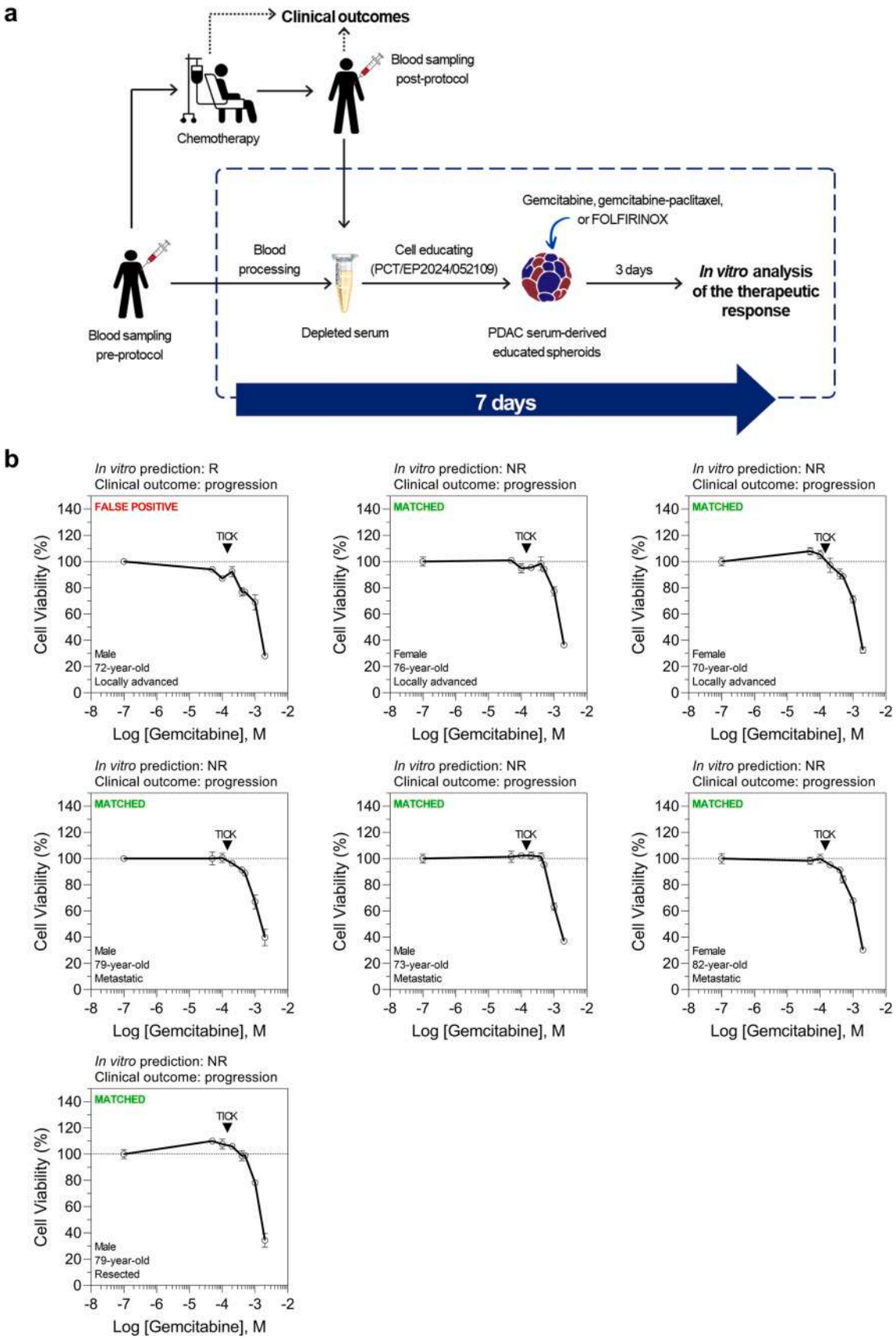

(caption on next page)

Fig. 4. Evaluation of the performance of PDAC patient serum-derived educated spheroids to reproduce the clinical outcomes to chemotherapies. (a) Schematic representation of the experimental workflow. Blood sera from PDAC patients were collected before the patient underwent a clinical treatment protocol or after the completion of the treatment protocol. PDAC patient serum-derived educated spheroids were generated and then treated with the same treatment as the one that he/she received in the clinic. A blind and unbiased *in vitro* analysis of the response was performed. The true therapeutic response to chemotherapies was determined using the TICK exclusion strategy. The full process from blood processing to final reports was 7 days. (b) Clinical outcomes and *in vitro* prediction responses to gemcitabine monotherapy. PDAC patient serum-derived educated spheroids from 7 PDAC patients were generated and then treated for 3 days with gemcitabine alone according to the clinical treatment protocol. Cell viability was measured to evaluate the effect of each treatment. A decrease in cell viability at or below the TICK value for each chemotherapy is considered an on-target effect, thereby confirming the true therapeutic efficacy of the drug. Results are expressed as mean % of cell viability ± *s*.e.m. Each condition was performed in technical triplicate.

providing critical insights to optimize future study design and determine sensitivity and specificity. Moreover, this work lays the foundation for continued collaboration with clinicians and regulatory authorities, with the long-term goal of developing a simple, non-invasive model that may ultimately improve patient care.

Although pancreatic stellate cells (PSCs) are the prototypical cancer-associated fibroblast (CAF) source in PDAC, our findings support the use of hepatic stellate cells (HSCs) as a practical and biologically relevant surrogate for stromal modeling in drug efficacy studies. Upon activation, HSCs adopt the same myofibroblastic CAF program as PSCs, characterized by α-SMA expression, collagen I deposition, and secretion of cytokines such as IL-6, CXCL12, and TGF-β [33]. These shared effector functions drive the hallmarks of stromal-mediated resistance, including matrix stiffening that impedes drug penetration, activation of survival signaling pathways in cancer cells, and recruitment of immunosuppressive myeloid populations that blunt immunotherapy responses [33]. Because these mechanisms represent conserved CAF-driven barriers across solid tumors rather than pancreas-specific phenomena, we believe that HSC-based models are sufficient to capture the critical stromal influences on therapeutic response. Furthermore, the established use of HSCs in fibrosis and drug screening research provides technical advantages, including reproducibility and accessibility, making them a robust system for evaluating stromal-targeted interventions before validation in PSC-specific contexts. The detection of collagen type I in our PDAC spheroids suggests that HSCs may substitute for PSCs by reproducing ECM-associated effects on drug response. This is further supported by the concordance between drug sensitivities observed in our PDAC models and reported clinical outcomes.

Pancreatic ductal adenocarcinoma patients often show poor response to standard chemotherapies. Indeed, gemcitabine monotherapy has an objective response rate of about 13 %, with most patients not achieving clinical benefit, and the disease progresses within 3 months [34]. Combination therapies like Gem-Pac and FOLFIRINOX improve outcomes. However, PDAC patients can develop resistance during treatment, and over 50 % of them may experience disease progression within 6 months [35,36]. These data highlight the urgent need for personalized models not only to predict treatment response but also to monitor it dynamically during therapy enabling early identification of drug resistance. The ability of our technology to establish a personalized chemogram from a simple blood sample provides a non-invasive and clinically practical tool to adjust or switch treatments promptly, potentially improving patient outcomes and avoiding ineffective therapies. Our results clearly support the feasibility and clinical relevance of this personalized approach. Moreover, they also highlight a critical factor that must be considered when implementing such strategies. Specifically, our data show that blood sampling for the generation of patient-specific chemogram should be performed within the week prior to initiating the treatment protocol. This timing is essential because PDAC is an extremely aggressive malignancy with highly dynamic tumor behavior, and delays between sampling and treatment initiation may result in chemogram profiles that no longer reflect the current tumor state. Indeed, rapid changes in tumor biology could lead to inaccurate predictions of therapeutic response if outdated serum samples are used. Thus, strict timing of sample collection is crucial to ensure that chemogram-guided treatment decisions are both relevant and effective. Our findings that spheroids generated using patient serum collected after treatment initiation produced results consistent with clinical outcomes further support the use of this personalized model to monitor dynamic treatment responses. This approach enables real-time assessment of therapeutic efficacy and provides a valuable tool for detecting emerging drug resistance. By reflecting the evolving tumor behavior during treatment, the model offers the opportunity to promptly adapt therapeutic protocols based on individualized response profiles. Such adaptability is particularly critical in PDAC, where rapid disease progression can limit the window for effective intervention.

We acknowledge the limitations of this study. First, the small sample size restricts the ability to draw definitive conclusions about the model's predictive performance regarding clinical outcomes. Second, among the patients evaluated, only one individual, a 72-year-old female with metastatic PDAC, demonstrated a positive clinical response to Gem-Pac. This isolated case, while encouraging, limits the generalizability of the findings and is insufficient to validate the model's predictive accuracy across a broader patient population. Nevertheless, and despite these limitations, this study represents the first attempt to provide evidence that a simple, non-invasive *in vitro* model, based on patient serum-derived educated spheroids and TICK exclusion strategy, can reflect clinical responses in PDAC. This approach opens new perspectives for the development of personalized treatment plans. We believe that our results will stimulate further research and encourage clinicians, the pharmaceutical industry, and healthcare organizations to support larger-scale studies aimed at validating the clinical utility of serum-derived educated spheroids in the management of PDAC.

Data statement

Results generated in this study are not publicly available. Methods related to this study will be shared on reasonable request with permission of PredictCan Biotechnologies SAS.

Ethics approval

Informed consent was obtained from all subjects and/or their legal guardian(s). The research protocol was conducted under French legal guidelines and fulfilled the requirements of the local institutional ethics committee. The study was approved by the "Direction Générale de la recherche et de l'innovation" (CODECOH, n°DC-2021–4779). This project does not involve the human person according to the legislation (article L1121–1 du code de la santé publique).

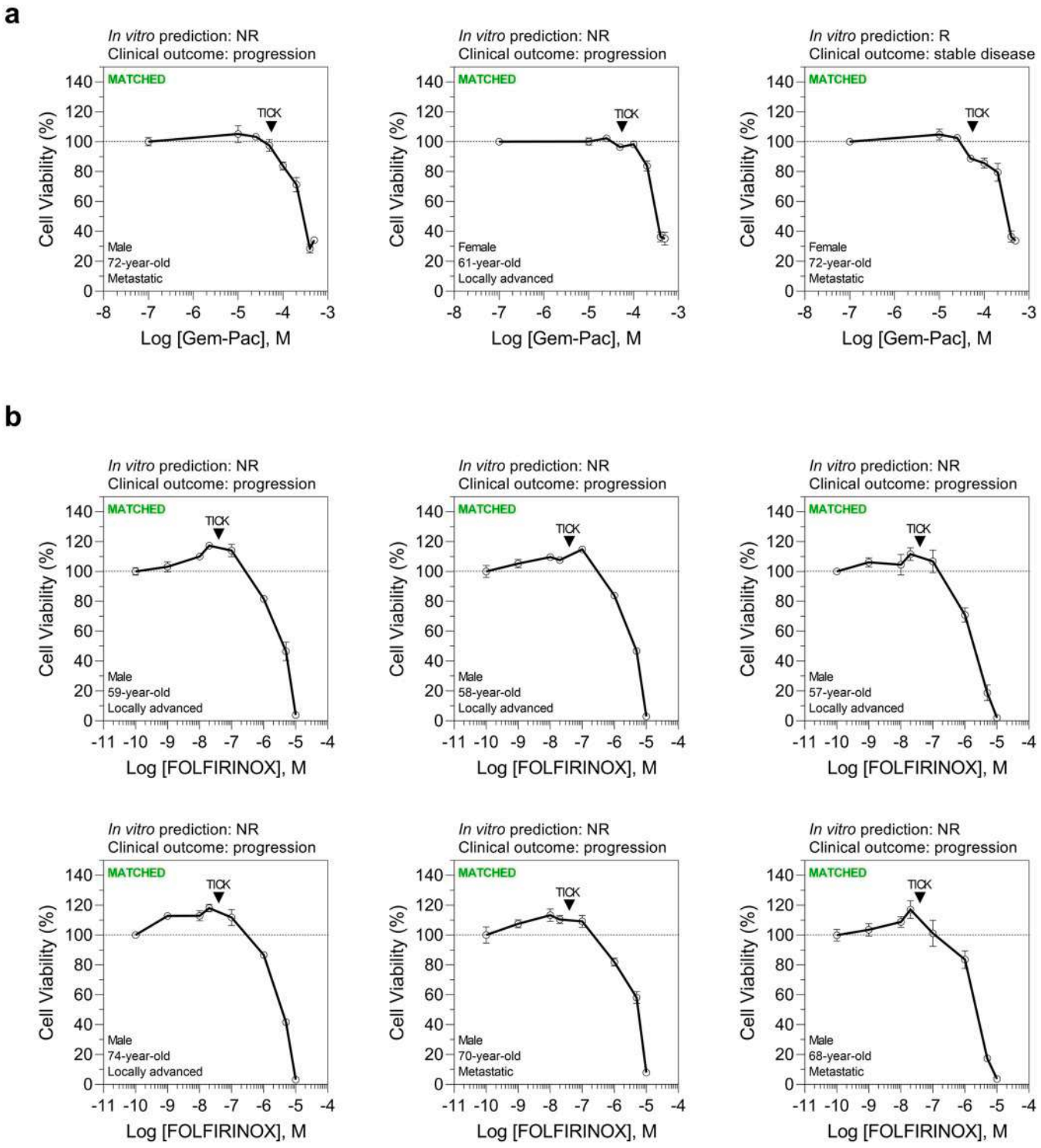

Fig. 5. Clinical outcomes and *in vitro* prediction responses to Gem-Pac and FOLFIRINOX. (a) PDAC patient serum-derived educated spheroids from 3 PDAC patients were generated and then treated with Gem-Pac according to the clinical treatment protocol. The true therapeutic efficacy was determined based on the TICK value for Gem-Pac. A decrease in cell viability at or below the TICK value for each chemotherapy is considered an on-target effect, thereby confirming the true therapeutic efficacy of the drug. Results are expressed as mean % of cell viability ± *s*.e.m. Each condition was performed in technical triplicate. (b) PDAC patient serum-derived educated spheroids from 6 PDAC patients were generated and then treated with FOLFIRINOX according to the clinical treatment protocol. The true therapeutic efficacy was determined based on the TICK value for FOLFIRINOX. A decrease in cell viability at or below the TICK value for each chemotherapy is considered an on-target effect confirming the true therapeutic efficacy of the drug. Results are expressed as mean % of cell viability ± *s*.e.m. Each condition was performed in technical triplicate.

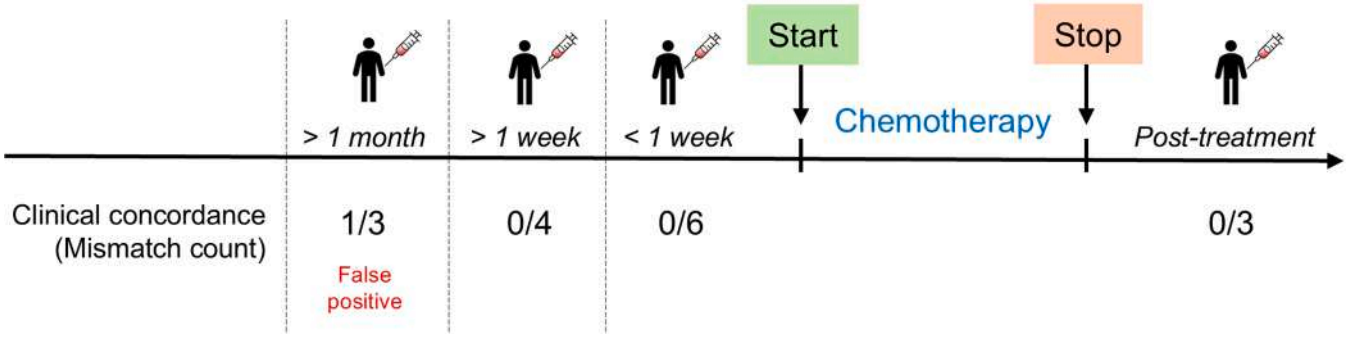

Fig. 6. Analysis of clinical concordance based on the timing of blood sampling. This scheme illustrates the assessment of predictive performance of PDAC serum-derived educated spheroids with respect to the timing of blood collection. Prediction accuracy was evaluated across different sampling times. Spheroids were derived from PDAC patients treated according to clinician-scheduled protocols with gemcitabine, Gem-Pac, or FOLFIRINOX. Among the 16 case studies analyzed (shown in Figs. 4 and 5), blood was collected more than one month before treatment initiation for 3 patients, more than one week before for 4 patients, and less than one week before for 6 patients. Three patients had blood collected after completion of their clinical protocol. Prediction accuracy was assessed by mismatch counts to determine concordance with clinical outcomes. Of the 16 cases, only one mismatch (a false positive) was observed in a 72-year-old male with locally advanced PDAC whose blood was collected more than one month before starting clinical treatment. Numbers report mismatch counts.

Funding support

This study was funded by the Region Occitanie and the French Government as part of the France 2030 Plan "Projets d'Innovation" DOS0222542/00 & DOS0222543/00.

CRediT authorship contribution statement

Sara Cherradi: Writing – review & editing, Supervision, Project administration, Investigation, Formal analysis. **Salomé Roux:** Writing – review & editing, Resources, Investigation, Formal analysis. **Marie Dupuy:** Writing – review & editing. **Eric Assenat:** Writing – review & editing. **Hong Tuan Duong:** Writing – original draft, Supervision, Formal analysis, Conceptualization.

Declaration of competing interest

Sara Cherradi, Salomé Roux, and Hong Tuan Duong. are employees of PredictCan Biotechnologies SAS. Sara Cherradi and Hong Tuan Duong are founders of PredictCan Biotechnologies SAS. The other authors have no competing interests.

Acknowledgments

This work is supported by the Etablissement Français du Sang Hauts de France-Normandie. We acknowledge the BACAP consortium: [1]Barbara Bournet, Cindy Canivet, Louis Buscail, Nicolas Carrère, Fabrice Muscari, Bertrand Suc, Rosine Guimbaud, Corinne Couteau, Marion Deslandres, Pascale Rivera, Anne-Pascale Laurenty, Nadim Fares, Karl Barange, Janick Selves, Anne Gomez-Brouchet. [2]Bertrand Napoléon, Bertrand Pujol, Fabien Fumex, Jérôme Desrame, Christine Lefort, Vincent Lepilliez, Rodica Gincul, Pascal Artru, Léa Clavel, Anne-Isabelle Lemaistre. [3]Laurent Palazzo;[4]Jérôme Cros;[5]Sarah Tubiana; [6]Nicolas Flori, Pierre Senesse, Pierre-Emmanuel Colombo, Emmanuelle Samail-Scalzi, Fabienne Portales, Sophie Gourgou, Claire Honfo Ga, Carine Plassot, Julien Fraisse, Frédéric Bibeau, Marc Ychou; [7]Pierre Guibert, Christelle de la Fouchardière, Matthieu Sarabi, Patrice Peyrat, Séverine Tabone-Eglinger, Caroline Renard; [8]Guillaume Piessen, Stéphanie Truant, Alain Saudemont, Guillaume Millet, Florence Renaud, Emmanuelle Leteurtre, Patrick Gele; [9]Eric Assenat, Jean-Michel Fabre, François-Régis Souche, Marie Dupuy, Anne-Marie Gorce-Dupuy, Jeanne Ramos; [10]Jean-François Seitz, Jean Hardwigsen, Emmanuelle Norguet-Monnereau, Philippe Grandval, Muriel Duluc, Dominique Figarella-Branger; [11]Véronique Vendrely, Clément Subtil, Eric Terrebonne, Jean-Frédéric Blanc, Etienne Buscail, Jean-Philippe Merlio; [12]Dominique Farges-Bancel, Jean-Marc Gornet, Daniela Geromin; [13]Geoffroy Vanbiervliet, Anne-Claire Frin, Delphine Ouvrier, Marie-Christine Saint-Paul; [14]Philippe Berthelémy, Chelbabi Fouad; [15]Stéphane Garcia, Nathalie Lesavre, Mohamed Gasmi, Marc Barthet; [16]Vanessa Cottet; [17]Cyrille Delpierre. [1]TheCHU and the University of Toulouse, Toulouse, France; [2]Jean Mermoz Hospital, Lyon, France; [3]Trocadéro Clinic, Paris, France; [4]The Department of Pathology, Beaujon Hospital and Paris 7 University, Clichy, France.[5]TheBiobank, Bichat Hospital and Paris 7 University, Paris, France; [6]The Cancer Institute and the University of Montpellier, Montpellier, France; [7]The Léon Bérard Cancer Center, Lyon, France;[8]The Department of Digestive Surgery, the CHU and the University of Lille, Lille, France;[9]The CHU and the University of Montpellier, Montpellier, France.[10]La Timone Hospital and the University of Marseille, Marseille, France;[11]The CHU and the University of Bordeaux, Bordeaux, France;[12] Saint Louis Hospital and Paris 7 Diderot University, Paris, France;[13] The CHU and the University of Nice, Nice, France;[14] Pau Hospital, Pau, France;[15] The CHU Nord Hospital and the University of Marseille, Marseille, France;[16] INSERM UMR866 and the University of Dijon, Dijon, France;[17] INSERM UMR1027 and the University of Toulouse, Toulouse France. We acknowledge the "Réseau d'Histologie Expérimentale de Montpellier" - RHEM facility for histology technics and expertise. RHEM facility is supported by SIRIC Montpellier Cancer Grant INCa_Inserm_DGOS_12553, REACT-EU (Recovery Assistance for Conditions générales du RHEM_IRCM Version 6 Page 7 / 9 Cohesion and the Territories of Europe), GIS FC3R whose funds managed by Inserm, IBiSA, Ligue contre le cancer and Occitanie Region.

References

[1] J. Ushio, A. Kanno, E. Ikeda, K. Ando, H. Nagai, T. Miwata, et al., Pancreatic ductal adenocarcinoma: epidemiology and risk factors, Diagn. (Basel) 11 (3) (2021).
[2] C. Hu, S.N. Hart, W.R. Bamlet, R.M. Moore, K. Nandakumar, B.W. Eckloff, et al., Prevalence of pathogenic mutations in cancer predisposition genes among pancreatic cancer patients, Cancer Epidemiol Biomark. Prev 25 (1) (2016) 207–211.
[3] D.B. Zhen, K.G. Rabe, S. Gallinger, S. Syngal, A.G. Schwartz, M.G. Goggins, et al., BRCA1, BRCA2, PALB2, and CDKN2A mutations in familial pancreatic cancer: a PACGENE study, Genet. Med. 17 (7) (2015) 569–577.
[4] K.Y. Elbanna, H.J. Jang, T.K. Kim, Imaging diagnosis and staging of pancreatic ductal adenocarcinoma: a comprehensive review, Insights. ImAging 11 (1) (2020) 58.
[5] T. Koltai, Earlier diagnosis of pancreatic cancer: is it possible? Cancers. (Basel) 15 (18) (2023).
[6] D.S. Swords, M.C. Mone, C. Zhang, A.P. Presson, S.J. Mulvihill, C.L. Scaife, Initial misdiagnosis of proximal pancreatic adenocarcinoma is associated with delay in diagnosis and advanced stage at presentation, J. Gastrointest. Surg. 19 (10) (2015) 1813–1821.
[7] O.T. Olaoba, M. Yang, T.I. Adelusi, T. Maidens, E.T. Kimchi, K.F. Staveley-O'Carroll, et al., Targeted therapy for highly desmoplastic and immunosuppressive

tumor microenvironment of pancreatic ductal adenocarcinoma, Cancers. (Basel) 16 (8) (2024).
[8] M. Dhir, M.S. Zenati, A. Hamad, A.D. Singhi, N. Bahary, M.E. Hogg, et al., FOLFIRINOX *Versus* gemcitabine/nab-paclitaxel for neoadjuvant treatment of resectable and borderline resectable pancreatic head adenocarcinoma, Ann. Surg. Oncol. 25 (7) (2018) 1896–1903.
[9] K. Abe, M. Kitago, Y. Kitagawa, A. Hirasawa, Hereditary pancreatic cancer, Int. J. Clin. Oncol. 26 (10) (2021) 1784–1792.
[10] S. Takeuchi, M. Doi, N. Ikari, M. Yamamoto, T. Furukawa, Mutations in BRCA1, BRCA2, and PALB2, and a panel of 50 cancer-associated genes in pancreatic ductal adenocarcinoma, Sci. Rep. 8 (1) (2018) 8105.
[11] M.A. Heinrich, A. Mostafa, J.P. Morton, L. Hawinkels, J. Prakash, Translating complexity and heterogeneity of pancreatic tumor: 3D *in vitro* to *in vivo* models, Adv. Drug Deliv. Rev. 174 (2021) 265–293.
[12] K. Peschke, H. Jakubowsky, A. Schafer, C. Maurer, S. Lange, F. Orben, et al., Identification of treatment-induced vulnerabilities in pancreatic cancer patients using functional model systems, EMBo Mol. Med. 14 (4) (2022) e14876.
[13] H.Y. Tanaka, T. Kurihara, T. Nakazawa, M. Matsusaki, A. Masamune, M.R. Kano, Heterotypic 3D pancreatic cancer model with tunable proportion of fibrotic elements, Biomaterials 251 (2020) 120077.
[14] H. Tiriac, P. Belleau, D.D. Engle, D. Plenker, A. Deschenes, T.D.D. Somerville, et al., Organoid profiling identifies common responders to chemotherapy in pancreatic cancer, Cancer Discov. 8 (9) (2018) 1112–1129.
[15] M.J. Ware, V. Keshishian, J.J. Law, J.C. Ho, C.A. Favela, P. Rees, et al., Generation of an *in vitro* 3D PDAC stroma rich spheroid model, Biomaterials 108 (2016) 129–142.
[16] B. Gundel, X. Liu, M. Lohr, R. Heuchel, Pancreatic ductal adenocarcinoma: preclinical *in vitro* and ex vivo models, Front. Cell Dev. Biol. 9 (2021) 741162.
[17] Y. Yu, G. Yang, H. Huang, Z. Fu, Z. Cao, L. Zheng, et al., Preclinical models of pancreatic ductal adenocarcinoma: challenges and opportunities in the era of precision medicine, J. Exp. Clin. Cancer Res. 40 (1) (2021) 8.
[18] L. Demyan, A.N. Habowski, D. Plenker, D.A. King, O.J. Standring, C. Tsang, et al., Pancreatic cancer patient-derived organoids can predict response to neoadjuvant chemotherapy, Ann. Surg. 276 (3) (2022) 450–462.
[19] K. Matsumoto, N. Fujimori, K. Ichihara, A. Takeno, M. Murakami, A. Ohno, et al., Patient-derived organoids of pancreatic ductal adenocarcinoma for subtype determination and clinical outcome prediction, J. Gastroenterol. 59 (7) (2024) 629–640.
[20] S.J. Hachey, A. Sobrino, J.G. Lee, M.D. Jafari, S.J. Klempner, E.J. Puttock, et al., A human vascularized microtumor model of patient-derived colorectal cancer recapitulates clinical disease, Transl. Res. 255 (2023) 97–108.
[21] S. Cherradi, S. Roux, M. Dupuy, S. Tabone-Eglinger, E. Tuaillon, M. Ziol, et al., Modelling hepatocellular carcinoma microenvironment phenotype to evaluate drug efficacy, Sci. Rep. 15 (1) (2025) 1179.
[22] S. Cherradi, N. Taulet, H.T. Duong, An original donor-dependent spheroid system for the prediction of idiosyncratic drug-induced liver injury risk, *In vitro* models (2023), https://doi.org/10.1007/s44164-023-00057-w.
[23] E. Darrigues, Z.A. Nima, R.J. Griffin, J.M. Anderson, A.S. Biris, A. Rodriguez, 3D cultures for modeling nanomaterial-based photothermal therapy, Nanoscale Horiz. 5 (3) (2020) 400–430.
[24] S. Lee, J. Lim, B. Kwak, Factors of bias in spheroid-based drug screening: fabrication method, spheroid size, and cell viability, Biomed. PharmacOther 192 (2025) 118597.
[25] A. Lin, C.J. Giuliano, A. Palladino, K.M. John, C. Abramowicz, M.L. Yuan, et al., Off-target toxicity is a common mechanism of action of cancer drugs undergoing clinical trials, Sci. Transl. Med. 11 (509) (2019).
[26] J. Timar, A. Uhlyarik, On-Target Side Effects of Targeted Therapeutics of Cancer, Pathol. Oncol. Res. 28 (2022) 1610694.
[27] A.E.J. Latenstein, L.G.M. van der Geest, B.A. Bonsing, B. Groot Koerkamp, N. Haj Mohammad, I. de Hingh, et al., Nationwide trends in incidence, treatment and survival of pancreatic ductal adenocarcinoma, Eur. J. Cancer 125 (2020) 83–93.
[28] J. Crimmin, T. Fulop, N.M.L. Battisti, Biological aspects of aging that influence response to anticancer treatments, Curr. Opin. Support. Palliat. Care 15 (1) (2021) 29–38.
[29] P. Gupta, R. Murad, L. Ling, Y. Zhang, K. Duong-Polk, S. Maganti, et al., The aging microenvironment as a determinant of immune exclusion and metastatic fate in pancreatic cancer, bioRxiv. (2025).
[30] M. Macchini, M. Chiaravalli, S. Zanon, U. Peretti, E. Mazza, L. Gianni, et al., Chemotherapy in elderly patients with pancreatic cancer: efficacy, feasibility and future perspectives, Cancer Treat. Rev. 72 (2019) 1–6.
[31] S. Roux, S. Cherradi, H.T. Duong, Uncovering the mechanism of troglitazone-mediated idiosyncratic drug-induced liver injury with individual-centric models, Arch. Toxicol. (2024).
[32] S. Roux, S. Cherradi, H.T. Duong, Exploiting the predictive power of educated spheroids to detect immune-mediated idiosyncratic drug-induced liver injury: the case of troglitazone, Front. Pharmacol. 15 (2024) 1378371.
[33] L. Kaps, D. Schuppan, Targeting cancer associated fibroblasts in liver fibrosis and liver cancer using nanocarriers, Cells 9 (9) (2020).
[34] P. Karasek, T. Skacel, I. Kocakova, O. Bednarik, L. Petruzelka, B. Melichar, et al., Gemcitabine monotherapy in patients with locally advanced or metastatic pancreatic cancer: a prospective observational study, Expert. Opin. PharmacOther 4 (4) (2003) 581–586.
[35] J. Prejac, D. Tomek Hamzic, N. Librenjak, I. Gorsic, D. Kekez, S. Plestina, The effectiveness of nab-paclitaxel plus gemcitabine and gemcitabine monotherapy in first-line metastatic pancreatic cancer treatment: a real-world evidence, Medicine 101 (39) (2022) e30566.
[36] B. Varzaru, R.A. Iacob, A.E. Croitoru, S.M. Iacob, C.E. Radu, S.M. Dumitrescu, et al., Real-life results of palliative chemotherapy in metastatic pancreatic ductal adenocarcinoma, Cancers. (Basel) 15 (13) (2023).